Small rotation angle measurement using an imaging method

Takamasa Suzuki†, Hideki Nakamura, John E. Greivenkamp*,and Osami Sasaki
Niigata University, Faculty of Engineering, 8050 Ikarashi 2, Niigata, 950-2181, JAPAN
*Optical Sciences Center, University of Arizona, Tucson, Arizona 85721, USA

ABSTRACT

A system of small rotation angle measurement based on the fringe projection is proposed and demonstrated. This system has potential for a broad range of uses and a robustness for the external disturbances, because it requires no coherent light. The setup is very simple and applicable to the automatic on-line measurement. Several measurements indicate a sensitivity of 3 arcsec.

Keywords: rotation angle measurement, image processing, fringe projection, on-line measurement

1. INTRODUCTION

Measurement of the rotation angle[1,2] involves the use of such established measuring devices as interferometers and autocollimators. While the former are extremely accurate, their use is usually limited, due to financial constrains, and the fact that they require an operating environment totally isolated from external disturbances. The latter, while being simple to use, take much longer to obtain the target-measurement. Therefore, they not suitable for automatic measurement.

The system we proposed is not based on either of the above method, but on what is referred to as optical image processing or fringe projection method[3]. Using Fourier transform (FT) method[4,5], we calculate the angle, from the relative phase shift of the viewed grating image. Although the method bears some resemblance to Moiré deflectmetry[6], it is unique, in that it does away with the need for coherent light source, expensive optical equipment, or the Moiré fringe, relying instead on single grating. Its insensitivity to external disturbances ensures that is operationally robust. Moreover, measurements require little or no fine tuning, thus making it ideally suited to automatic on-line measurement. Detection sensitivity is also tunable, by varying the spatial frequency of the grating, or the distance between the test target and the CCD camera.

2. PRINCIPLE

2.1 Mathematical formula

Figure 1 illustrates how the system measures the relative angle between the reference mirror (M1) and the object mirror (M2) which rotates around the point of origin (O). A grating image projected simultaneously onto M1 and M2 is reflected to, and observed on the viewing plane. The viewed grating images reflected by M1 and M2 are called reference image and object image, respectively, in this paper. If M2 slightly rotates by θ, the reference image shifts by s against the object image. The shift s represented by

†Correspondence: E-mail: takamasa@eng.niigata-u.ac.jp;
Telephone / FAX: +81-25-262-7215

Part of the SPIE Conference on Three-Dimensional Imaging, Optical Metrology, and Inspection V • Boston, Massachusetts • September 1999
SPIE Vol. 3835 • 0277-786X/99/$10.00

$$s = d\tan 2\theta + x_0 \tan\theta \tan 2\theta \quad (1)$$

is a function of viewing distance d, rotation angle θ, and x_0 the x-coordinate of the grating. Since the x_0 is much smaller than d, and θ is very small, the second term of Eq. (1) can be neglected. Then, the rotation angle θ is given by

$$\theta = \frac{1}{2}\tan^{-1}\left(\frac{s}{d}\right). \quad (2)$$

We measure the phase difference Δα between the reference and the object image to calculate the shift s. The phases α_1 and α_2 of the reference and the object image are detected by means of the FT method, respectively. The Δα is given by

$$\Delta\alpha = \alpha_1 - \alpha_2. \quad (3)$$

The shift s is then calculated by

$$s = \frac{P}{2\pi}\Delta\alpha, \quad (4)$$

where P is the grating pitch. The rotation angle θ is given by

$$\theta = \frac{1}{2}\tan^{-1}\phi, \quad (5)$$

where

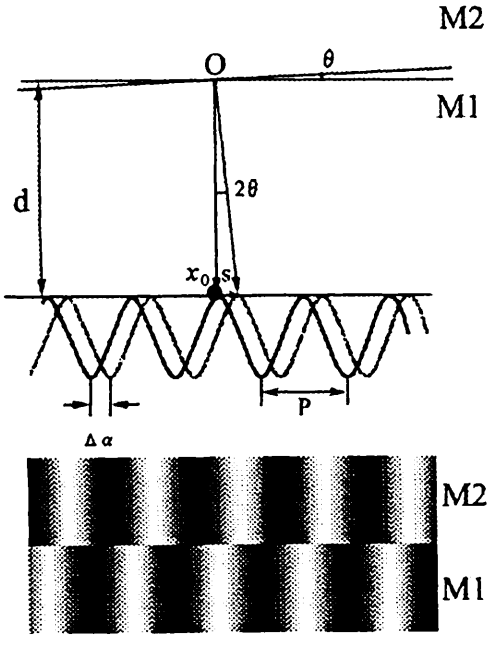

Fig. 1 Principle of the measurement. M1, Reference mirror; M2, Object mirror; s, Fringe shift; Δα, Phase difference; P, Grating pitch; d, Viewing distance.

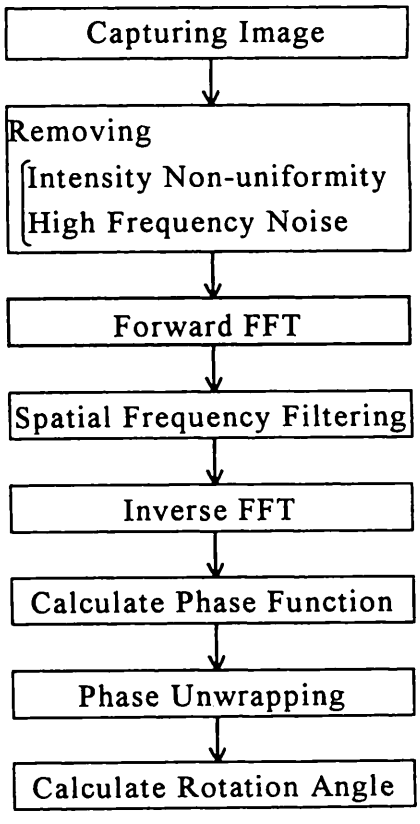

Fig. 2 Flow chart of the image processing.

$$\phi = \frac{P}{2\pi d}\Delta\alpha \quad . \tag{6}$$

Since the amount of phase shift is the function of the grating pitch P and the viewing distance d, resolution can be adjusted by changing P and d.

2.2 Signal processing

The flow chart shown in Fig. 2 details the major steps in our process. After capturing reflected image, some area to be processed is selected. The selected image is filtered to remove the non-uniformity on intensity and the high frequency noise. Phase calculation is made by the FT method. In that method, the frequency components are calculated from the preprocessed image with the Fast Fourier Transform (FFT). After the frequency filtering, the inverse FFT is carried out to obtain the phase of the grating image. The FT method is applied to the reference and the object image. Then, the phase difference $\Delta\alpha$ is detected and rotation angle θ is calculated by the formula described above.

2.3 Error analysis

In this system, we have to consider two kinds of error sources. One of them is the error in the phase difference $\Delta\alpha$. It comes from the resolution of the FT method. The detected phases α_1 and α_2 have some errors of $\Delta\alpha_1$ and $\Delta\alpha_2$. These errors, however, take almost same values if the pixel size of the CCD camera is small enough, because two gratings have a same spatial frequency, gratings are not deformed but just shift, and CCD image sensor takes images with a same sampling frequency. Therefore, these errors are reduced to zero with the subtraction shown in Eq. (3). The other is a systematic error depending on the viewing distance d and the grating period P. This error is given by

$$\Delta\phi = \frac{\partial\phi}{\partial P}\Delta P + \frac{\partial\phi}{\partial d}\Delta d = \frac{\Delta\alpha}{2\pi d}\left(\Delta P - \frac{P}{d}\Delta d\right) \quad . \tag{7}$$

The maximum value $\Delta\phi$ is

$$\Delta\phi\big|_{max} = \Delta\phi\big|_{\Delta\alpha=\pm\pi} = \pm\frac{1}{2d}\left(\Delta P - \frac{P}{d}\Delta d\right) \quad . \tag{8}$$

This error can be reduced to be zero with the calibration of the viewing distance d.

2.4 Calibration of the viewing distance

We assume that M2 is pushed by the micrometer-head positioned L distance from the point of origin as shown in Fig. 3. If

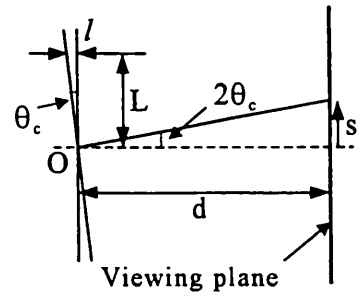

Fig. 3 Calibration of the viewing distance.

the travel pitch of the micrometer-head is l, the rotation angle θ is given by

$$\theta = \tan^{-1}\left(\frac{l}{L}\right). \tag{9}$$

We increase l to be l_c where the fringe shift s equals to the grating pitch P. It is easy to realize this condition, because the phase shift is 2π and there is no phase difference between the reference image and the object image. Combining Eqs. (2) and (9) under the above condition, we can obtain

$$\theta_c = \tan^{-1}\left(\frac{l_c}{L}\right) = \frac{1}{2}\tan^{-1}\left(\frac{P}{d}\right). \tag{10}$$

Consequently, the calibrated viewing distance d_c is given by

$$d_c = \frac{P}{\tan\left\{2\tan^{-1}\left(\frac{l_c}{L}\right)\right\}}. \tag{11}$$

3. EXPERIMENT

3.1 Experimental setup

The experimental setup shown in Fig. 4 consists of a computer-generated grating image, a CCD camera with an imaging lens and a computer. The object rotates around the point of origin, by means of a micrometer-head positioned L=80 mm distance from the point of origin, where "Forward" means push-out and "Reverse" means drawback of the mirror. The grating image reflected by the mirror is captured by the CCD camera through a small aperture that is upper-center of the grating. The captured images are then processed by a computer. The calibrated viewing distance d_c was 280 mm. No special lighting effects were employed, during the conduct of this experiment. We relied, instead, upon what was available naturally.

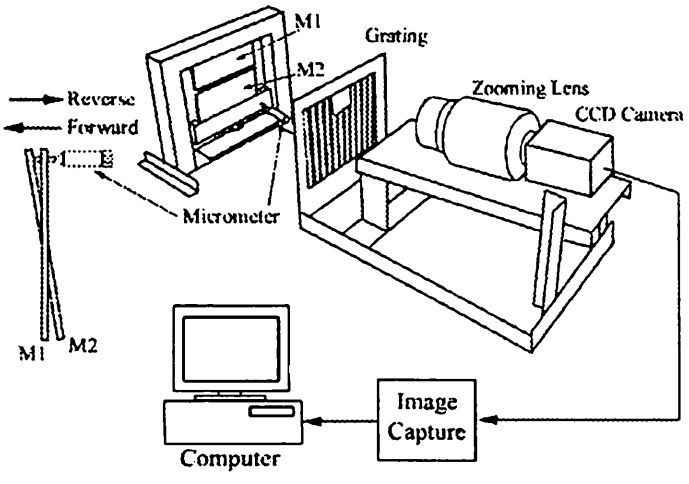

Fig. 4 Experimental setup.

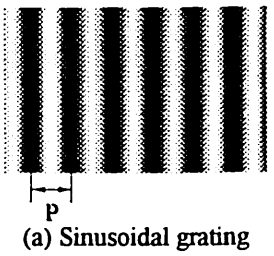

(a) Sinusoidal grating

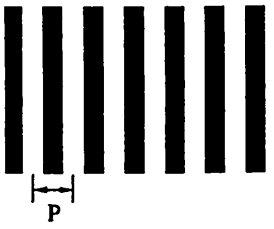

(b) Binary grating

Fig. 5 Grating images used in the experiments.

Since this system is prototype, it uses two mirrors as a reference and a object in this experiments. Actually, however, this system requires just one object mirror if the object image is captured before it rotates. We used two kinds of grating the sinusoidal grating and the binary grating as shown in Fig. 5. They were printed with a laser-beam printer of 600 dpi.

3.2 Display of the image processing

Figure 6 serves to explain how images are processed. We made familiar Window format to display images and results. The original images reflected by M1 and M2 are displayed in the upper and lower areas of the Source Window, respectively. The images used in phase analysis are gotten of Source Window and displayed in the Object Window. The phase function obtained, is shown in the Process Window. Parameters such as grating pitch and viewing distance are displayed in the I/O field. Measurement results are also displayed in the I/O field.

3.3 Results

At first, we examined required cyclic numbers of the grating for realizing a good measurement as a preliminary measurement. Several calculations were made with a simulation. Figure 7 shows that good measurement accuracy can be achieved when we use more than six of cyclic number. The magnification of Fig. 7 in the region more than six of cyclic number is shown in Fig. 8. It indicates that the measurement error is less than 0.1 arcsec if we select more than ten cyclic numbers of grating.

We made simulations to confirm the measurement accuracy. Figure 9 is the result obtained with the sinusoidal grating. The x-axis shows the displacement of M2 driven by the micrometer-head. In this case, the travel pitch was 1 μm. The results detected by our method shows a good agreement with a theoretical line. Measurement error was 0.0154 arcsec in rms. The

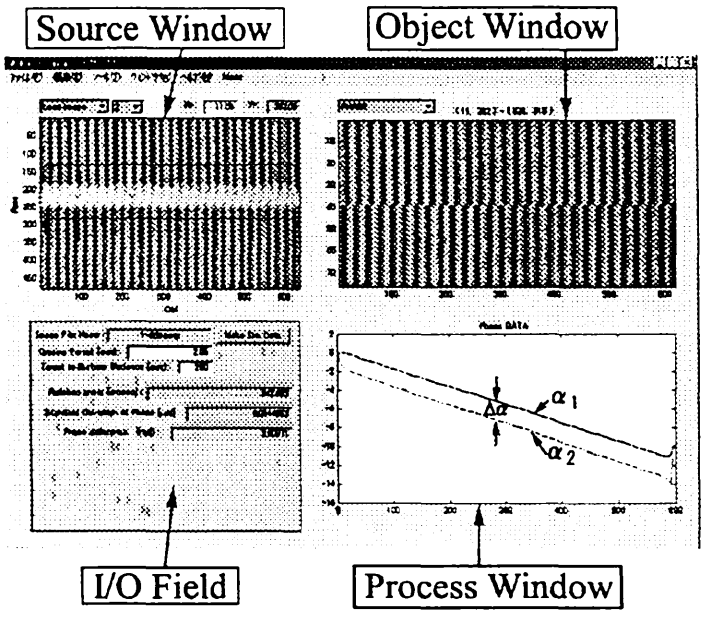

Fig. 6 Display of the image processing.

result obtained with the binary grating is shown in Fig. 10. Periodic measurement error was detected in this simulation. It is considered that the frequency resolution of the FT method was not so good for the binary grating.

We used the micrometer-head to rotate M2 around the point of origin, noting each 10 μm shift, whether forward or backward. Major results that are measured with a sinusoidal grating and a binary grating are shown in Figs. 11 and 12, respectively. The grating pitch in both instances was 2.06 mm. The varied range of the rotation angle was 500 arcsec in this experiments. When the sinusoidal grating was used, measurement errors both in forward and reverse direction were under 2 arcsec in rms. When the binary grating was used, the errors were around 3 arcsec in rms. The periodic error observed in the simulation disappeared in the experiment. Because the optical system forms a kind of low-pass filter and the binary grating

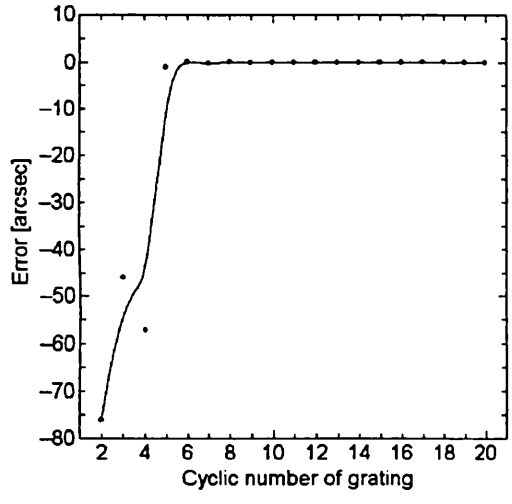

Fig. 7 Measurement error depending on the cyclic numbers of the grating.

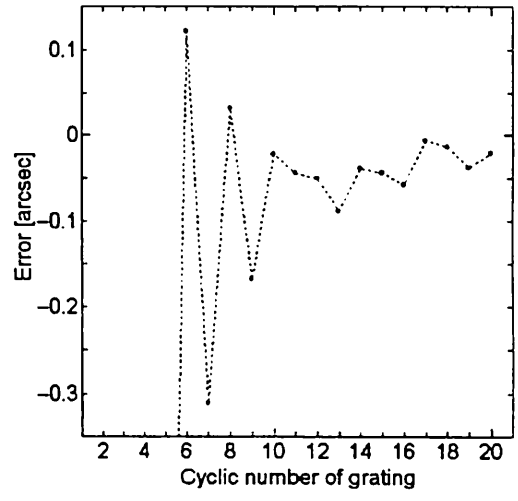

Fig. 8 Magnification of the part of Fig. 6.

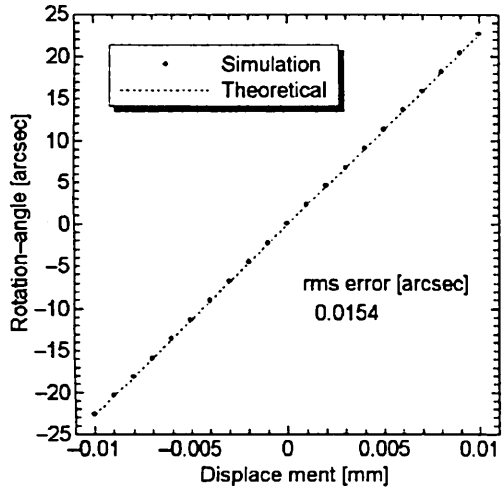

Fig. 9 Measurement error calculated by a simulation with the sinusoidal grating.

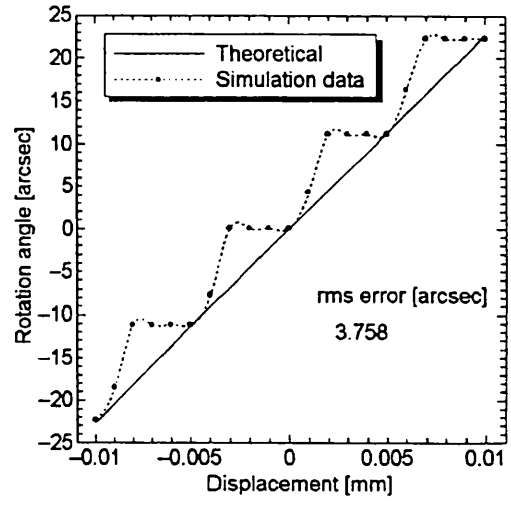

Fig. 10 Measurement error calculated by a simulation with the binary grating.

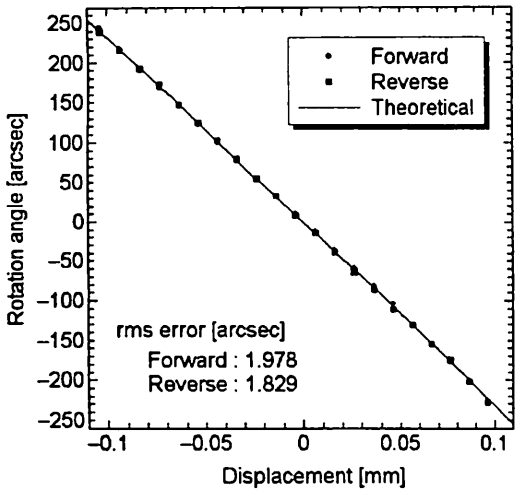

Fig. 11 Rotation angle measurement with a sinusoidal grating. Travel pitch of the micrometer-head is 10 μm.

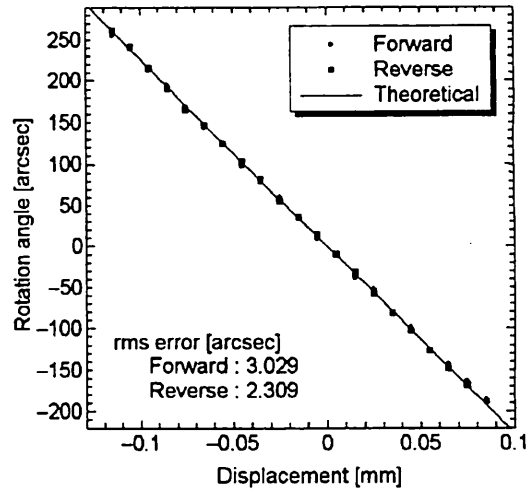

Fig. 12 Rotation angle measurement with a sinusoidal grating. Travel pitch of the micrometer-head is 10 μm.

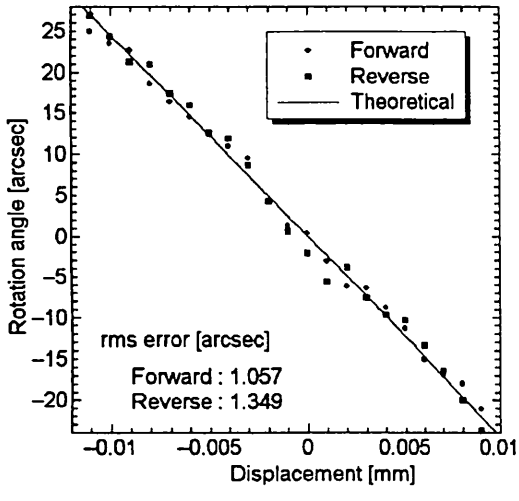

Fig. 13 Rotation angle measurement with a sinusoidal grating. Travel pitch of the micrometer-head is 1 μm.

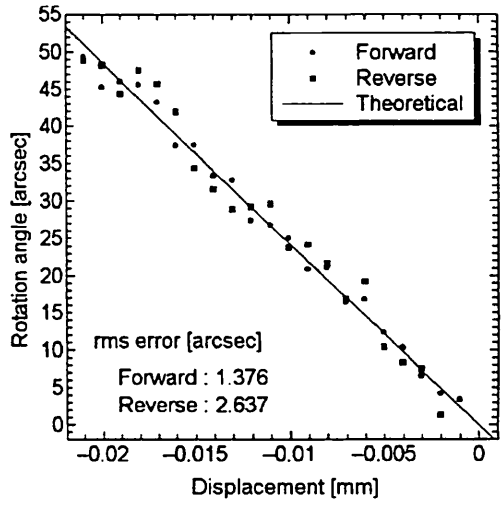

Fig. 14 Rotation angle measurement with a binary grating. Travel pitch of the micrometer-head is 1 μm.

has been changed to quasi-sinusoidal grating.

The results obtained when the object mirror M2 was driven with the travel pitch of 1 μm are shown in Figs. 13 and 14. The varied range of the rotation angle was 50 arcsec. When the sinusoidal grating was used, measurement error was under 2 arcsec in both forward and reverse direction. When the binary grating was used, measurement error was under 3 arcsec in rms. We think these errors come from not only our measurement system but also the mirror-rotating system that uses micrometer-head.

4. CONCLUSION

In conclusion, we have proposed and demonstrated small rotation angle measurement system. Our system has a lot of advantages. It is simple because it uses non-coherent light source, computer generated grating transparency, and CCD camera. Since it does not require coherent light source, it is insensitive to external disturbance and works with rough alignment. In the theoretical analysis, we clarified the error sources and made some computer simulations to check the measurement accuracy. Required cyclic number of the grating is six and the measurement error was very small.

In the experiments, we measured several rotation-angles of the object mirror that was driven by the micrometer-head. Measured angles agreed well with the theoretical ones. They indicate a measurement accuracy of 3 arcsec. We think that precise mirror-rotating system is required to estimate the actual measurement error in our system.

REFERENCES

1) J. Z. Malacara, "Angle, Distance Curvature, and Focal Length Measurements," Chap. 18, in Optical Shop Testing, D. Malacara, Ed., (John Wiley and Sons, New York, 1992), pp. 718-720.
2) P. Shi and E. Stijns, "New optical method for measuring small-angle rotations," Appl. Opt. 27,4342-4344 (1988).
3) K. Leonhardt, U. Droste, and H. J. Tiziani, "Microshape and rough-surface analysis by fringe projection," Appl. Opt. 33, 7477-7488 (1994).
4) T. Mitsuo, H. Ina, and S. Kobayashi, "Fourier-transform method of fringe pattern analysis for computer-based topography and interferometry," J. Opt. Soc. Am., 72, 156-160 (1982).
5) T. Mitsuo, K. Mutoh, "Fourier transform profilometry for the automatic measurement of 3-D object shapes," Appl. Opt. 22, 3977-3982 (1983).
6) O. Kafri and J. Glatt, "Moiré deflectmtry: a ray deflection approach to optical testing," Opt. Eng., 24, 944-960 (1985).